Theme IV - Understanding Seismicity Catalogs and their Problems

Earthquake Location Accuracy

Stephan Husen[1] • Jeanne L. Hardebeck[2]

1. Swiss Seismological Service, ETH Zurich
2. United States Geological Survey

Contents

Abstract Earthquake location catalogs are not an exact representation of the true earthquake locations. They contain random error, for example from errors in the arrival time picks, as well as systematic biases. The most important source of systematic errors in earthquake locations is the inherent dependence of earthquake locations on the assumed seismic velocity structure of the Earth. Random errors may be accounted for in formal uncertainty estimates, but systematic biases are not, and they must be considered based on knowledge about how the earthquakes were located. In this article we discuss earthquake location methods and methods for estimating formal uncertainties; we consider systematic biases in earthquake location catalogs; and we give readers guidance on how to identify good-quality earthquake locations.

1 Motivation

Statistical seismology strives to quantify, test, and understand the spatial-temporal behavior of earthquakes. However, the spatial-temporal properties of earthquakes cannot be studied directly; one must instead study the spatial-temporal properties of earthquake catalogs. The applicability of any particular statistical result to the real Earth depends in part on the extent to which the utilized catalog accurately represents the real earthquake properties. Therefore, when undertaking a statistical study using an earthquake catalog, it is vital to understand the original purpose and limitations of the catalog and how these limitations may affect the study's results.

Consider, for example, the Parkfield segment of the San Andreas Fault, the focus of many studies (e.g. *Bakun et al.* 2005), and a location where numerous earthquake catalogs have been generated for different purposes. Some research goals at Parkfield depend on characterizing the distances between earthquakes, such as *Rubin and Gillard's* (2000) study of the scaling of the distances between consecutive events with the magnitude of the first event. These research goals are best served by earthquake catalogs that have been created with the purpose of precisely locating the events relative to one another, with less concern about their absolute position in space. *Rubin and Gillard* (2000) therefore used a catalog based on waveform cross-correlation, which uses small shifts in arrival times to precisely constrain the relative locations of nearby events. Other research goals are dependent on knowing the absolute locations of earthquakes, a major example being the SAFOD project's goal of drilling through the San Andreas at the location of a repeating earthquake sequence. This requires an earthquake catalog that has been created with the purpose of accurately determining the absolute locations of the earthquakes, with less concern about their relative locations. Catalogs based on careful modeling of the seismic velocity structure at Parkfield (e.g., *Zhang et al.* 2009) should provide the best absolute locations.

Earthquakes can be located using different techniques ranging from standard linearized techniques to probabilistic techniques employing direct-searches of the solution space, from single-event locations to joint multiple-event locations, from absolute locations to relative locations. Each technique relies on certain

assumptions and has its strengths and weaknesses. Knowing these is important to understand the limitations of a given earthquake catalog. Catalog earthquake locations and origin times, like all quantitative data, have uncertainty due to random errors in the basic observations used to derive them. In addition to random location errors, earthquake catalogs may include location artifacts and systematic location biases, which are not reflected in the formal uncertainties provided with the catalog. The common source of most systematic location errors is the fundamental problem that estimates of earthquake locations, earthquake origin times, and the Earth's seismic velocity structure are inherently coupled. To find the correct earthquake locations requires the correct velocity structure, which is of course never exactly known, creating tradeoffs between seismic velocity models and earthquake parameters.

In this article, we discuss the most commonly used methods for locating earthquakes, methods for estimating the formal uncertainty representing the random errors, and common artifacts related to the coupling of earthquake locations to seismic velocity structure. We present some general "rules of thumb" to help catalog users identify good quality earthquake locations, and discuss common issues in local, regional, and global scale catalogs. To assist users in identifying the appropriate catalog for their particular study, we also discuss the advantages and disadvantages of catalogs located using single-event and relative-location techniques.

For this article, we assume that the reader is familiar with seismic waves and raytracing, such as the material covered in *Shearer* (1999) or *Lay and Wallace* (1995). The reader should also have some familiarity with seismic networks (e.g., *Lee and Stewart* 1981) and geophysical inverse techniques (e.g., *Menke* 1989, *Tarantola* 2005). However, the reader need not be an expert in these fields.

2 Location Techniques

2.1 A coupled, inherently nonlinear problem

An earthquake location specifies the place and time of occurrence of energy release from a seismic event. In combination with a measure of the size a location provides a concise description of the most important characteristics of an earthquake. The location may refer to the earthquake's epicenter, hypocenter, or centroid, or to another observed or calculated property of the earthquake that can be spatially or temporarily localized. An earthquake location can be absolute or relative. An absolute earthquake location is computed or specified within a fixed, geographic system and a fixed time base (e.g., Coordinated Universal Time (UTC)); a relative earthquake location is determined or specified with respect to another spatio-temporal object (e.g., an earthquake or explosion) which itself may have an unknown or an uncertain absolute location.

Because earthquakes take place deep in the Earth, their source locations must be inferred from observations that are recorded at stations located only at one side of

the earthquake (e.g., at the Earth's surface). This unfavorable geometry makes the determination of focal depth often difficult because rays are mainly upgoing (for local earthquakes) or downgoing (for regional and global earthquakes). An earthquake location is usually determined by the match or misfit between observed arrival times of seismic phases at seismic stations, and predictions of these arrival times for different source locations using a given model of seismic velocities, which is usually assumed to be a more or less exact representation of the true velocity structure. Hence, the process of determining an earthquake location can be seen as an inverse problem with four unknowns (spatial coordinates of the hypocenter location and origin time). The location that yields the smallest misfit between observed and predicted arrival times defines the hypocenter location.

For a given model of slowness $u(\mathbf{x})$ (inverse of seismic velocity) and source location $x_{srce}(\mathbf{x})$ the arrival time t_{obs} at a station with coordinates $x_{stat}(\mathbf{x})$ can be expressed as

$$t_{obs} = t_0 + \int_{x_{srce}}^{x_{stat}} u(\mathbf{x})ds \tag{1}$$

where $\mathbf{x}$ denotes a vector of spatial coordinates sampling the ray path and t_0 denotes origin time. Equation (1) is nonlinear since a change in the source location changes the ray path over which the integral is computed. Consequently, earthquake location, which maps arrival times into spatial coordinates and origin time, is inherently a nonlinear problem. Similarly, a change in the slowness model $u(\mathbf{x})$ in equation (1) will change arrival time, and, therefore, the hypocenter location. This is referred to as the coupled hypocenter-velocity problem (*Thurber* 1992). Since the seismic velocity structure of the Earth is unknown, computation of a single earthquake location would require determining the slowness model $u(\mathbf{x})$ as well. This is, of course, impossible and, consequently, the slowness model $u(\mathbf{x})$ is fixed during the computation of a single earthquake location. The *a priori* slowness model may be constrained, for example, by seismic refraction studies. For a large set of well-constrained earthquakes, however, the coupled hypocenter-velocity problem can be solved simultaneously (e.g., *Kissling* 1988, *Thurber* 1992).

2.2 Linear and nonlinear methods

The earliest, formal earthquake locations using arrival time information from seismic phases applied direct-search procedures such as graphical methods (*Milne* 1886) or simple grid-searches (*Reid* 1910). One of the graphical methods described by *Milne* (1886) can be seen as a generalization of using circles based on *S-P* arrival times, in which the radii of the circles is given by the corresponding *S-P* arrival time. In the 1970s digital computers allowed the use of linearized, iterative methods based mainly on *Geiger's* method (1912). Well-known examples are Hypo71 (*Lee and Lahr* 1975) or HYPOELLIPSE (*Lahr* 1989). Increasing computing power over the last decades has made large-scale, grid and stochastic direct searches feasible for earthquake locations (e.g., *Sambridge and Kennett* 1986, *Lomax et al.* 2000).

The term "nonlinear" is used ambiguously in geophysics to refer to linearized-iterated and to nonlinear methods. Here, we use the term to refer to global search

methods that do not use partial derivatives because linearized methods can also account for nonlinearity by iterating on the linearized solution.

Linearized methods in earthquake location are based on a Taylor series expansion of equation (1) around some prior estimate (or guess). Using only the first two terms of the Taylor series a linear relationship for arrival time is obtained. By combining all available arrival time observations for a single earthquake location a vector-matrix equation in the form

$$\mathbf{A}\mathbf{x} = \mathbf{d} \tag{2}$$

can be obtained, in which matrix $\mathbf{A}$ relates the adjustments of the hypocentral parameters (vector $\mathbf{x}$) to the vector $\mathbf{d}$ of misfits. Equation (2) can be solved using standard linear algebraic methods (*Menke* 1989). Since the original earthquake location problem is nonlinear, the linearized method needs to be iterated by using the result of the previous step as prior estimate for the next iteration until some pre-defined convergence criteria is met. Linearized methods produce a single, best-fit hypocenter and origin time location, and associated, linearly-estimated uncertainties, such as a multi-dimensional, normally distributed confidence ellipsoid centered on the best-fit hypocenter and origin time. This linearized solution, however, can be a poor representation of the complete solution, and it may be unstable when the complete solution is irregular or has multiple solutions due to insufficient or outlier data (e.g., *Husen et al.* 2003, *Lomax et al.* 2008). Because linearized methods do not involve large-scale searches they are computationally fast and, therefore, often the primary location method in routine earthquake location for cataloging by seismic networks. On the downside, the solution of linearized location methods depends on the choice of the prior estimate and, therefore, can be stuck in a local minimum.

Nonlinear location methods do not require the computation of partial derivatives. Instead, they are based on deterministic or stochastic searches, which may be exhaustive or directed and evolutionary. Because of that they are often referred to as direct-search location methods (*Lomax et al.* 2008). These methods explore or map functions that can be simply the root-mean-square (RMS) misfit (*Nelson and Vidale* 1990, *Husen and Kissling* 2001) or more sophisticated likelihood functions as given, for example, by *Lomax et al.* (2008). When these searches gather and retain information globally throughout the prior probability density function (pdf), they can produce a complete location pdf (*Tarantola and Valette* 1982, *Moser et al.* 1992, *Wittlinger et al.* 1993, *Lomax et al.* 2000). Otherwise, these searches may determine a global or local maximum of the location pdf, or may explore the neighborhood around these optimal points to locally estimate the pdf and obtain uncertainty information. The searches used in nonlinear location methods can be grouped into regular, deterministic searches, directed searches, and importance sampling (*Lomax et al.* 2008). Regular deterministic searches include grid-searches, nested grid-searches, and stochastic, "crude" Monte-Carlo searches (e.g., *Sambridge and Mosegaard* 2002). Since they use global and well-distributed sampling of the model space these searches can estimate the complete location pdf. They are, however, computationally demanding for problems with many unknowns, large model spaces or time-consuming forward calculations. Directed, stochastic search techniques include evolutionary, adaptive global search methods such as the genetic

algorithm (e.g., *Sambridge and Drijkoningen* 1992) and simulated annealing (e.g., *Kirkpatrick et al.* 1983). Most of these methods were developed for optimization or the identification of some very good solutions, which is equivalent to identifying a global or local maximum of the location pdf. In general, these methods do not explore the prior pdf in a manner that can produce complete, probabilistic solutions to inverse problems. Nevertheless, directed searches are useful for earthquake location because of their efficiency (e.g., *Sambridge and Gallagher* 1993). Importance sampling tries to choose a sampling density which follows the target function as closely as possible to allow an efficient sampling of the complete, probabilistic solution. The challenge of importance sampling lies in the fact that the target function is unknown, and consequently the optimum importance sampling distribution cannot be determined *a priori*. The oct-tree importance sampling, for example, has been proven to allow an efficient and reliable sampling of the complete probabilistic solution of earthquake location problem (*Lomax et al.* 2008, *Lomax and Curtis* 2001). It uses recursive subdivision and sampling of rectangular cells in a 3-D space to generate a cascade structure of sampled cells, such that the spatial density of the sampled cells follows the target pdf values. This oct-tree structure will have a larger number of smaller cells in areas of higher probability (lower misfit) relative to areas of lower pdf values. Oct-tree sampling has been implemented in the software package NonLinLoc to efficiently compute the complete, probabilistic solution to the earthquake location problem. It is increasingly applied to earthquake location in research and routine operations (e.g., *Lomax* 2005, *Lomax et al.* 2001, *Husen and Smith* 2004, *Husen et al.* 2003).

In summary, two classes of methods exist to solve the earthquake location problem. Iterative, linearized methods solve the problem by the use of partial derivatives and matrix inversion. They have the advantage of being computationally fast and they provide reliable solutions for well-constrained earthquake locations. They have the disadvantage that their solution depends on the quality of the initial guess and they can be unstable for poorly-constrained earthquake locations. Nonlinear or direct-search methods solve the earthquake location problem by sampling either the entire or only parts of the solution space. They have the advantage of obtaining a more complete solution with uncertainties as compared to the linearized methods and do not rely on the quality of initial guess. However, they can be computationally expensive.

2.3 Single-event, joint hypocentral determination, and relative location methods

Earthquakes are often located one at a time using arrival times from a set of stations that recorded the event. This procedure is often referred to as single-event location, and both linearized and nonlinear location methods can be used. The resulting location is absolute within a fixed, geographic system and a fixed time base. The location is independent of the location of other earthquakes and depends only on the observed arrival times and the seismic velocities used. Single-event location is usually still the preferred method for locating earthquakes, particular in routine earthquake location, as the underlying theory is reasonably well understood and the computational burden is low.

Instead of locating earthquakes one at a time, a set of earthquakes can be located jointly. In general, this is referred to as joint hypocenter determination (JHD) (e.g., *Douglas* 1967, *Kissling* 1988, *Pujol* 2000). JHD methods are usually linearized methods as the high dimensionality of the problem makes direct-search solutions difficult and computationally demanding. Similar to single-event location, JHD uses arrival times of seismic phases determined at seismic stations and the resulting locations are absolute. To reduce the effects of errors in the travel time model, JHD allows the use of static station corrections based either on travel time residuals (*Pujol* 1992) or by explicitly treating them as unknowns in the inverse problem (*Kissling* 1988). The station correction is a constant time added to all of the modeled travel-times to that station, and this accounts for unmodeled velocity structure along the common ray path below the station. The source-specific station term (SSST) technique replaces the single static correction at each station with station terms that vary as a function of source location (*Richards-Dinger and Shearer* 2000). For large data sets JHD can be used to detect systematic errors related to arrival time data or station parameters (location and timing) by investigating station specific travel time distributions or by comparing station corrections to local geology (e.g., *Kissling* 1988, *Maurer et al.* 2010). Although not strictly considered to be JHD methods, the simultaneous inversion for hypocenters and seismic velocities, as done in local earthquake tomography (e.g., *Thurber* 1993) or for the computation of a minimum 1-D model (*Kissling et al.* 1994), can be considered as such. More importantly, only the simultaneous inversion for hypocenters and seismic velocities is a proper solution to the coupled hypocenter-velocity problem, as traditional JHD does not allow inverting for seismic velocities. Consequently, hypocenter locations obtained by JHD can still be affected by systematic errors due to unmodeled velocity structure.

A set of earthquakes can be located relative to a master event or relative to each other. The former is usually called master-event location (e.g., *Deichmann and Garcia-Fernandez* 1992), whereas the latter is known as double-difference (DD) earthquake location (e.g., *Waldhauser and Ellsworth* 2000). The resulting locations are relative either to a master event in the case of master-event location or to each other in the case of DD earthquake location. In the case of master-event location, information on absolute locations depends on the absolute location of the master event. DD earthquake location can resolve absolute locations but the accuracy depends on the accuracy to which the true seismic velocities are known, similar to single-event location (*Menke and Schaff* 2004). As in JHD, both methods are linearized as the high dimensionality of the problem makes direct-search solutions difficult and computationally demanding.

Master-event location uses travel time residuals computed for the master event as station corrections to locate all other events, the so-called slave events. Least-square adjustments are computed using the relative travel time residuals. As a consequence, the relative locations computed this way are a function of travel-time differences between master and slave events and of the seismic velocity in the source region. Because the relative travel time residuals are smaller than the absolute travel time residuals, the improvement in consistency of the relative locations is mainly due to the fact of adjusting these smaller residuals (*Deichmann and Giardini* 2009). Master-event location relies on the assumption that errors in

the velocity model are the same for observation from two events at the same station. This assumption is usually valid for event-station distances that are large compared to inter-event distances. Consequently, master-event location can only be applied for a set of earthquakes within a restricted volume.

DD earthquake location relates the residual between observed and calculated differential travel time between two events to the distance between the two events (*Waldhauser and Ellsworth* 2000). Using the appropriate slowness vector at the source and origin time for each event, a system of linear equations in the form

$$\mathbf{WAm} = \mathbf{Wd} \tag{3}$$

can be created, where $\mathbf{A}$ defines a matrix of size M x $4N$ (M, number of double-difference observations; N, number of events) containing the partial derivatives, $\mathbf{d}$ is the data vector, $\mathbf{m}$ is a vector of length $4N$ containing the changes in hypocentral parameters, and $\mathbf{W}$ is a diagonal matrix to weight each equation. The matrix $\mathbf{A}$ is highly sparse, as each equation links together only two events. If one event is poorly linked to all other events, matrix $\mathbf{A}$ becomes ill conditioned, and the solution to equation (3) may become numerically unstable. This can be improved by using only events that are well linked to other events (*Waldhauser and Ellsworth* 2000). In general, this can be achieved by only allowing event pairs, which have more than a minimal number of observations (at least eight since the number of unknowns for one pair of events is eight).

With the DD method, a network is built in which each event is linked to its nearest neighbors through travel time differences observed at common stations. It differs from other JHD methods in that no station corrections are necessary, because unmodeled velocity structure is directly removed by using double-differences. This works best if the ray paths from two events to the same station are nearly identical. Hence, DD earthquake location works best if events are densely distributed (compared to average station spacing) and observed at a large number of stations. The strength of DD earthquake location lies in the fact that is uses travel time differences, which can be measured with a high precision using waveform cross-correlation methods (e.g., *Rowe et al.* 2002, *Schaff et al.* 2004). By using these cross-correlation methods, uncertainties in determining travel-time differences are greatly reduced. Theory and tests with synthetic data show that differential arrival time data also contain information on absolute earthquake location (*Waldhauser and Ellsworth* 2000, *Wolfe* 2002, *Menke and Schaff* 2004). Thus, DD earthquake location can resolve, to a certain extent, absolute earthquake locations. The performance depends, however, also on the knowledge of the true velocity structures as in the case for single-event earthquake locations (*Menke and Schaff* 2004).

3 Uncertainty and Artifacts

Uncertainties in earthquake locations are dominated by three factors (e.g., *Pavlis* 1986):

1. measurement errors of seismic arrival times,
2. modeling errors of calculated travel times,

3. nonlinearity of the earthquake location problem.

The latter is only relevant for linearized, least square solutions; direct-search methods (as discussed in section 2.2) do not require linearization of the earthquake location problem, and as such they are not affected by errors due to nonlinearity. The other two types of errors are relevant for linearized and direct-search methods. Measurement errors of arrival times are always present and stem from a number of sources, including signal-to-noise ratio and dominant frequency of the arriving phase. These errors lead to a relative location scatter around the true earthquake location. Hence, they define the *precision* of an earthquake location. In the earthquake location problem they can be treated from a purely statistical point of view to derive the well-known error ellipsoids, as described in section 3.1. Therefore, we will refer to these errors as *formal errors* of the earthquake location problem. Modeling errors of calculated travel times are mostly dominated by the quality of the seismic velocity model used to calculate them; the precision of the method used to calculate the travel times for a given velocity model plays only a minor role. It is well known that modeling errors of calculated travel times lead to systematic biases in earthquake location (e.g., *Jordan and Sverdrup* 1981, *Thurber* 1992, *Billings et al.* 1994a). Hence, these errors define the *accuracy* of an earthquake location. Proper handling of modeling errors of calculated travel times is difficult in earthquake location, mostly because the error is unknown. Among modeling errors of calculated travel times, other systematic errors, such as incorrect station coordinates or phase misidentification, can lead to a systematic bias in earthquake locations.

In the following we will explain in more detail how *precision* and *accuracy* can be assessed during the process of computing an earthquake location. We will also discuss how to assess them for earthquake catalogs that do not contain uncertainty information. To illustrate the problems in earthquake location we will provide a number of examples using real data.

3.1 Precision in earthquake locations or formal uncertainty estimates

Measurement errors of seismic arrival times

The arrival of a seismic phase at a station is usually marked by a change in the amplitude and frequency content of the seismic signal (Fig. 1). As any seismic signal is affected by a certain level of noise and the phase arrival is not characterized by a delta pulse, the arrival time of a seismic phase is uncertain. Surprisingly, the description of how to derive seismic arrival times and their uncertainties has received little attention in the literature. The general approach is to assign individual weights to each arrival time based on some (often subjective) criteria (e.g., *Buland* 1976). These weights are then used in locating the earthquake. This approach, however, provides only a qualitative assessment of measurement errors; it does not provide information on the statistical properties of the errors. This information is needed to compute the formal uncertainty estimates, as described below. In principle, it can be obtained by analyzing arrival times that have been picked by different analysts for the same data set, or by analyzing arrival times that have been picked by a single analyst for a data set with similar

epicenters (*Zeiler and Velasco* 2009). Often, these values are also taken as *a priori* information based on past experience. A more physical, consistent formulation in determining these measurement errors can only be achieved by a probabilistic point of view, in which the observation uncertainty is directly related to the measured arrival time (e.g., *Bormann et al.* 2002, *Diehl et al.* 2009b). In a probabilistic point of view, the onset of a seismic phase is interpreted as a probabilistic function $P_a(t)$, where the arrival time is expressed as the most likely time t_A, with $P_a(t) =$ Max(P_a) (Fig. 1). The measurement error is then given by the earliest and latest possible time for the phase onset t_E and t_L, respectively, where the likelihood for the onset is approaching zero. Hence $P_a(t_E) \geq 0$ and $P_a(t_L) \geq 0$. In practice, t_L can be defined as the time when the signal amplitude exceeds an *a priori* defined noise level (e.g. 1.5 times pre-signal amplitude; grey band in Fig. 1). A definition of t_E is more difficult since it is usually hidden in the noise; t_E can be defined, for example, where the slope of a tangent fitted to the slope of the signal approaches zero (dashed line in Fig. 1) A typical function to express the onset of a seismic phase would be a normal distribution centered on t_A (Fig. 1). For such a function, t_E and t_L would be symmetric around t_A. In this case, the process of determining t_A would require picking t_E and t_L first; t_A is then simply defined as the time in the middle between t_E and t_L. This approach may not be realistic but it is consistent with theory, in which errors are assumed to be Gaussian distributed. Although more complete, the process of determining t_A, t_E, and t_L is laborious and often not practical for routine operations. Therefore, a simple quality indication or, at best, a simple normal distribution is used to represent measurement errors of seismic arrival times. In many cases these simplified data uncertainty estimates will lead to bias or increased error in the resulting event locations.

Although the principles described above apply for both P- and S-wave arrivals, determination of the arrival time of an S-phase is more difficult. This is due to the fact that the S-wave arrival represents a secondary arrival, which arrives in the coda of the P-wave. As a consequence, the signal-to-noise ratio is much larger for S-wave arrivals. Moreover, S-wave arrivals can be preceded by converted phases, which are difficult to identify on single-component stations or on unrotated components (e.g., *Diehl et al.* 2009a). As a consequence, S-wave arrivals should only be picked on three-component stations, preferably on rotated components. Automatic procedures to determine arrival times for P- and S-wave arrivals are often solely restricted to the determination of arrival times (e.g., *Allen* 1978, *Baer and Kradolfer* 1987); information on uncertainties is usually not provided. Nevertheless, recent approaches have demonstrated the use of automated, quality-weighted phase picking for regional tomography models (*Di Stefano et al.* 2006, *Diehl et al.* 2009b). However, the application of such methods to routine earthquake locations needs to be tested, as a large percentage of low-quality arrival times is rejected. This does not pose a problem for earthquakes recorded at a large number of high-quality stations but can be problematic for earthquakes recorded at a small number of stations, as some of the rejected arrival times may close an important azimuthal gap. Hence, these observations provide important constraints on the earthquake location. Determination of seismic arrival times can be significantly improved and measurement errors can be significantly decreased by using semi-automated approaches using waveform cross-correlation techniques (e.g.,

Rowe et al. 2002). Obviously, these methods work best for data sets with a large percentage of similar waveforms.
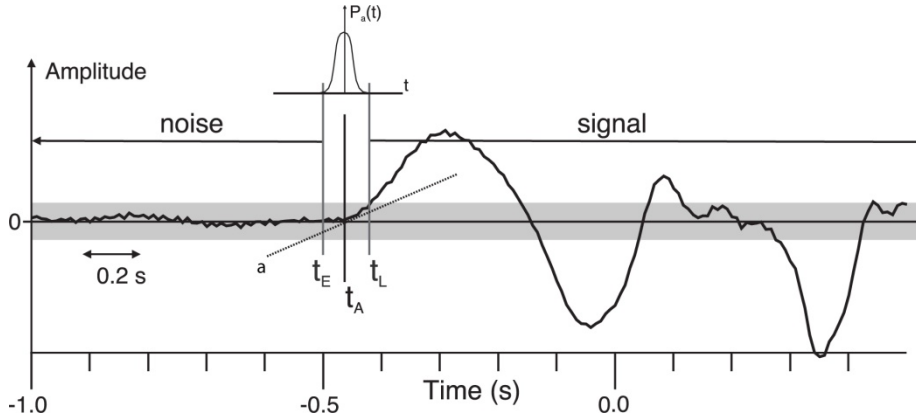
Fig. 1. Short segment of a seismic signal showing the arrival of a P-phase recorded at station BNALP of the Swiss Digital Seismic Network at a distance of about 200 km for a ML= 5.3 earthquake in northern Italy. The most likely arrival time is marked with t_A; t_E and t_L mark time of the earliest and latest possible arrival, respectively, defining the measurement error (uncertainty). Function $P_a(t)$ denotes a possible normal distribution depicting the probability of the arrival time. Grey band marks the level of 1.5 times pre-signal amplitude used to define t_L. Dashed line 'a' denotes a tangent fitted to the slope of the sgnals used to define t_E. See text for more details.

Methods to compute formal uncertainty estimates

In linearized earthquake location, confidence regions on the hypocenter, epicenter and focal depth can be computed under certain assumptions and using different types of statistics. The assumptions made are (e.g., *Boyd and Snoke* 1984):

1. measurement errors of seismic arrival times are uncorrelated and follow a normal distribution with a zero mean and a variance σ^2; and
2. the travel time functions $t_{obs}(\mathbf{x})$ as defined in equation (1) are locally linear near the hypocenter location.

These assumptions lead to confidence regions that are elliptical (linear) in shape and normal distributed. Depending on the knowledge of the variance σ^2 one of two types of statistics are used to compute the size of the confidence region:

1. If the variance σ^2 is unknown the F statistic is used (*Flinn* 1965, *Jordan and Sverdrup* 1981).
2. If the variance σ^2 is known the χ^2 statistic is used (*Evernden* 1969).

In the situation where the variance σ^2 is unknown, an estimate, S^2, is used; S^2 is derived from the residual vector $\mathbf{d}$ of equation (2) and the number of degrees of freedom (*Boyd and Snoke* 1984). The usefulness of such an approach is limited as

in the presence of velocity model inaccuracy the variance σ^2 will no longer represent the measurement errors of seismic arrival times.

Location algorithm	Statistic	Confidence level (%)		
		Hypocentral	Epicentral	Depth
HypoEllipse	χ^2	68	83	94
Hypo71	none	n/a	n/a	68*
HypoInverse	none	32	n/a	68*

Table 1. Error statistics and confidence levels used by different location algorithms (after *Boyd and Snoke* (1984)). The confidence level in depth for Hypo71 and HypoInverse (marked with *) was computed using a χ^2 value of 1.00.

Different linearized location algorithms use different statistics and confidence levels to compute confidence regions or location uncertainties (Table 1). From the location algorithms shown in Table 1 only HypoEllipse (*Lahr* 1989) uses a proper error statistic. Only HypoEllipse and HypoInverse compute a joint hypocentral confidence region. For HypoEllipse confidence regions for epicenter and depth are derived from the joint hypocentral confidence region by projecting the joint hypocentral error ellipsoid onto the corresponding regions and by scaling the major axis with the corresponding ratios of the χ^2 value for the different degrees of freedom (*Lahr* 1989). This results in confidence levels that are larger than the 68% joint hypocentral confidence region (*Boyd and Snoke* 1984). HypoInverse (*Klein* 2002) uses the square root of the eigenvalues of the covariance matrix to compute the major axes of the joint hypocentral error ellipsoid, which corresponds to a 32% confidence level. The horizontal error and the vertical error are simplified errors derived from the lengths and directions of the principal axes of the error ellipsoid by projection onto the corresponding axis (*Klein* 2002). HypoInverse also does not correctly subtract the four variables from the degree of freedom, and therefore underestimates the uncertainty. Hypo71 (*Lee and Lahr* 1975) uses the square root of the sum of the estimated latitude and longitude variances to define the error in epicenter. Neither of these methods to compute uncertainties in epicenter has inherent statistical interpretations since, geometrically, an axis projection is in general not the same as the projection of the ellipse or ellipsoid (*Boyd and Snoke* 1984). The depth error estimate computed by HypoInverse or Hypo71 can be given a statistical interpretation by assuming a χ^2 value of 1.00 (*Boyd and Snoke* 1984). To facilitate the comparison of the uncertainty estimates between the different location algorithms, *Boyd and Snoke* (1984) derived factors to scale location uncertainties between the different algorithms. It should be noted that the interpretation of confidence levels in terms of standard deviations is only valid for one dimensional confidence levels, e.g. for focal depth, but not for joint confidence levels, e.g. for epicenter.

All three programs allow scaling of the size of the derived location uncertainties using the final data fit, e.g., travel time residuals. Only HypoEllipse would allow the use of an *a priori* estimated measurement error for scaling. Scaling of the location uncertainties using the final data fit, however, may lead to smaller location uncertainties for well constrained earthquake locations with a lower number of

observations since it is easier to fit a few observations than a large number of observations. This is, of course, contradicting the fact that earthquake locations are usually better constrained using a large number of observations. Furthermore, the scaling of the location uncertainties using the final data fit assumes that errors in the velocity model are normal distributed, which is not adequate and may even yield misleading results (*Pavlis* 1986).

Formal uncertainty estimates computed for DD earthquake locations are usually a few orders of magnitude smaller than the corresponding uncertainties for single-event locations (e.g., *Waldhauser and Ellsworth* 2000). This is reflecting mainly the higher precision of relative arrival time measurements, in particular if cross-correlation methods are used to measure them. As for single-event locations, these lower uncertainties for relative locations do not provide information on the accuracy of the earthquake locations. For DD earthquake locations, these depend as well on the quality of the velocity model used for relocation. Furthermore, DD earthquake locations can be affected by variations in station distribution. These uncertainties cannot be quantified directly for DD earthquake location but can be quantified using statistical tests such as the jackknife method (*Waldhauser and Ellsworth* 2000).
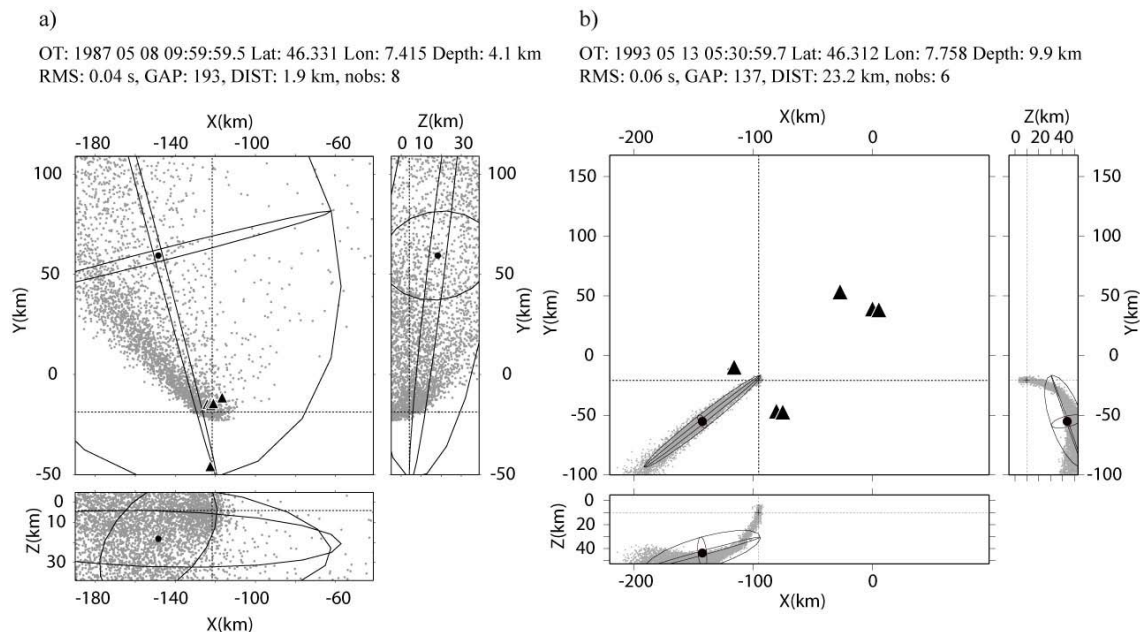
As direct-search methods sample the entire solution space they allow us to compute confidence regions that can be non-ellipsoidal in shape (e.g., *Wilcock and Toomey* 1991). Depending on the functions that are mapped these confidence regions may represent simple misfit surfaces (e.g., *Billings et al.* 1994b, *Husen and Kissling* 2001) or confidence regions, in the case of the posterior probability density function (e.g., *Moser et al.* 1992, *Husen et al.* 2003). Fig. 2 shows an example of a relatively well-constrained hypocenter location of a small earthquake recorded by the Swiss Digital Seismic Network. Another way of displaying the location pdf is by showing so-called density scatterplots (*Lomax et al.* 2000, *Husen et al.* 2003, *Husen and Smith* 2004). These density plots are obtained by drawing a subset of samples from the entire set of points sampled during the search, with the number of samples proportional the probability. Hence, a region with a higher probability to contain the earthquake location is shown by a higher number of samples (Fig. 2). From the set of pdf samples, traditional or Gaussian uncertainty estimates can be computed such as the expectation hypocenter location or the 68% confidence ellipsoid (Fig. 2). These estimates can be seen as the results from linearized earthquake location. The density scatterplots represent the geometrical properties of the location pdf, which represents most completely the result of probabilistic, direct, global-search methodologies. As can be inferred from Fig. 3, the shape of the location pdf can be quite complicated and irregular, and it is not adequately represented by traditional Gaussian uncertainty estimates. More examples of how the location pdf may look can be found, for example, in *Lomax et al.* (2008b).
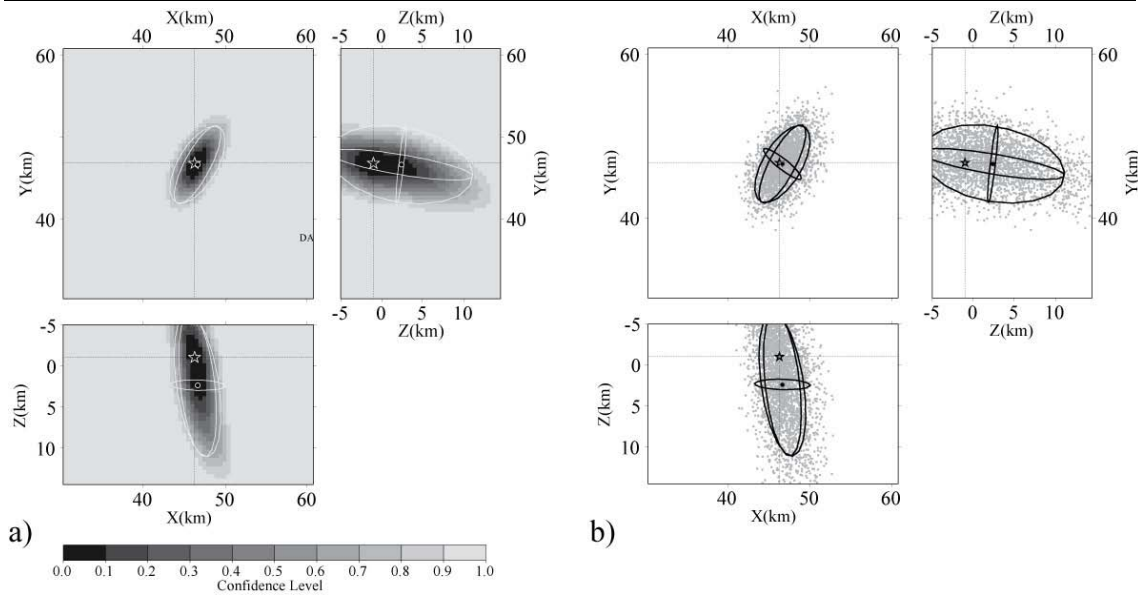
Fig. 2. Probabilistic location uncertainties of a relatively well-constrained earthquake location displayed as a) confidence regions and b) density scatterplots. Maximum likelihood hypocenter locations are marked with by stars; expectation hypocenter locations are marked by circles. Error ellipsoid corresponds to the 68% confidence ellipsoid as computed from the samples of the location pdf. Modified from *Husen et al.* (2003).

It is important to note that only the probabilistic approach of *Tarantola and Valette* (1982) and as implemented by *Moser et al.* (1992) and *Lomax et al.* (2000) can separate the errors due to the velocity model and those due to the measurement of arrival times. All other approaches, either linearized or based on direct-search methods, describe the errors using a joint error distribution, such as a generalized Gaussian (e.g., *Billings et al.* 1994a). Theoretically, the formulation of *Tarantola and Valette* (1982) would allow a proper handling of the uncertainties associated with velocity model errors and measurement errors. For reasons of simplicity and to derive the location pdf analytically the *a priori* density functions describing the state of knowledge of the velocity model and measurement errors had to be assumed to be Gaussian. However, *Pavlis* (1986) found that it may not be adequate to represent the velocity model error as a Gaussian distribution with zero mean and that, under this assumption, misleading results can be obtained. Therefore all location methods suffer from an inappropriate handling of velocity model errors, which will be discussed in more detail in section 3.2.

a)

OT: 1987 05 08 09:59:59.5 Lat: 46.331 Lon: 7.415 Depth: 4.1 km
RMS: 0.04 s, GAP: 193, DIST: 1.9 km, nobs: 8

b)

OT: 1993 05 13 05:30:59.7 Lat: 46.312 Lon: 7.758 Depth: 9.9 km
RMS: 0.06 s, GAP: 137, DIST: 23.2 km, nobs: 6

Fig. 3. Density scatterplots of two poorly-constrained earthquake locations recorded by the Swiss Digital Seismic Network. Maximum likelihood hypocenter locations are marked by the intersection of dashed lines. Black circles mark expectation hypocenter locations. Error ellipsoid corresponds to the 68% confidence ellipsoid as computed from the samples of the location pdf. Black triangles denote station locations. Note that for these location pdf the error ellipsoid does not present an adequate representation of the location uncertainties. Modified from *Husen et al.* (2003).

Uncertainty estimates based on network criteria

As outlined above, all earthquake location methods provide uncertainty estimates under certain assumptions. Nevertheless, many earthquake catalogs either do not provide this information or, if provided, the information is based on linearized location methods with rather unreliable uncertainty estimates. Earthquake location studies based on direct-search methods are still a minority. Because of that people have tried to assess the reliability of earthquake locations using so-called network criteria. These criteria usually include the following measures, which can be derived from the geometry of the stations that recorded the earthquake or from the data fit:

1. nobs = number of observations (P- and S-wave arrival times);
2. GAP = greatest azimuthal angle without observation;
3. DIST = distance to the closest station;
4. RMS = root mean square of the travel time residuals for the final earthquake location.

Using these criteria several studies tried to establish "rules of thumb" that would describe well-constrained hypocenter locations (see for example *Gomberg et al.*

1990, *Bondar et al.* 2004 and references therein). Some of these well-known rules are:

1. You need a GAP < 180°for a well constrained earthquake location (*Kissling* 1988);
2. You need at least eight travel time arrivals, of which at least one is an S-wave arrival, and at least one was reported from a station within a focal depth's distance from the epicenter for a well constrained hypocenter location (*Chatelain et al.* 1980);
3. A correctly timed S-wave arrival recorded within 1.4 focal depth's distance from the epicenter provides a unique constraint on focal depth (*Gomberg et al.* 1990).

These rules of thumb try to mimic the fact that for a stable earthquake location, matrix $\mathbf{A}$ in equation (2) needs to have a low condition number, i.e. the columns of matrix $\mathbf{A}$ need to be linearly independent (see *Lee and Stewart* 1981, page 137). The elements of matrix $\mathbf{A}$ are the spatial derivatives of the travel times from the trial hypocenter to the stations. These depend on the seismic velocity and the take-off angles of the seismic rays at the hypocenter. As the take-off angles depend on the geometry of the hypocenter with respect to the stations, the geometry of the observing stations plays a critical role in how well constrained an earthquake location is. To minimize the condition number of matrix $\mathbf{A}$ columns need to be linearly independent. This can be achieved, for example, by ensuring a wide range of take-off angles, which is most likely achieved by using a large number of arrival time observations at different distances. The requirement of one arrival from a station within a focal depth's distance ensures that there is at least one up-going ray.

Focal depth is generally less well constrained than epicenter. This can be understood by considering the properties of matrix $\mathbf{A}$. Since the first column of matrix $\mathbf{A}$ contains the partial derivatives with respect to the origin time, which are always one, the chances that the fourth column, which contains the partial derivatives with respect to focal depth, becomes a multiple of the first column is high. This can happen in a situation where all stations are located at a similar distance to the epicenter or if the P-wave arrivals are coming from the same refractor in a layered model. Similarly, the well-known tradeoff between origin time and focal depth can be explained by this linear dependence between the first and fourth column of matrix $\mathbf{A}$. Fixing focal depth, as done by many linearized location methods, will remove this tradeoff and lower the condition number of matrix $\mathbf{A}$, thus yielding a more stable inversion. The use of depth phases (*pP*, *pwP*, *sP*) will greatly improve focal depth estimates as their partial derivatives differ significantly in magnitude from those of the direct P-arrival (*Engdahl* 2006). Furthermore, the tradeoff between origin time and focal depth is avoided as the partial derivates of depth phases are opposite in sign to the direct P-arrival.

It is important to note that the rules of thumb discussed above only refer to the precision of an earthquake location. They usually do not give estimates on the accuracy of an earthquake location. To assess the accuracy of an earthquake location, sources with known locations, such as explosions or mine blasts, need to

be used. For example, *Bondar et al.* (2004) used data from exceptionally well-located earthquakes and nuclear explosions to establish epicenter accuracy based on seismic network criteria for different scales (local, regional, teleseismic). Their results indicate that rather strict criteria are needed to obtain high-quality earthquake locations: e.g., for local network locations 10 or more stations, a GAP < 110°, DIST < 30 km, and a secondary azimuthal gap < 160° are needed to obtain a location accuracy of 5 km with a 95% confidence level. The study of *Bondar et al.* (2004) does not give similar estimates for focal depth. Hence, it would be best for a given catalog to estimate these parameters using the approach of *Bondar et al.* (2004) but including focal depth as well.

The effect of adding S-wave arrivals to location uncertainties

S-wave arrivals provide an important constraint on focal depth of an earthquake, in particular if they are observed at a station within 1.4 focal depth's distance (*Gomberg et al.* 1990). Within this distance the partial derivative of an S-wave arrival with respect to focal depth provides a unique constraint due to the lower seismic velocities of the S-waves. An S-wave arrival does not only provide an important constraint on focal depth but also on location uncertainties. As can be seen in Fig. 4 the use of S-wave arrivals dramatically reduces the uncertainty in focal depth; without S-wave observations, the focal depth of the earthquake is nearly unconstrained despite the fact of a relatively small GAP (GAP=144°) and a station within focal depth distance (DIST=23.7 km). Focal depth is unconstrained for this earthquake because the range of station distances is relatively poor and, consequently, all the rays show similar take-off angles (Fig. 4). The situation is greatly improved by adding S-wave arrivals due to the lower seismic velocities of the S-waves. Compared to the location uncertainties the corresponding shift in epicenter and focal depth is relatively small indicating that the main effect of adding S-wave arrivals for this earthquake was a decrease in the location uncertainties. It is important to note, that adding S-wave arrivals does not necessarily improve the location accuracy. First, picking of S-wave arrivals is complicated by converted phases which can arrive shortly before the actual onset of the S-wave. Such a phase misidentification can yield a systematic bias in the earthquake location which cannot even be detected due to the apparent decrease in the formal uncertainties (*Gomberg et al.* 1990). Second, the assumption of using a constant P- to S-wave velocity ratio to locate an earthquake in the absence of an S-wave velocity model can also lead to a location bias (*Maurer and Kradolfer* 1996). In both cases, an earthquake location obtained using P-wave arrivals only will provide an improved location accuracy without a potential bias; however, using only P-waves also yields a lower precision.

Fig. 4 is also a nice example on how unreliable the earthquake's RMS value is to assess location quality. Although RMS is a factor of three lower, the location obtained using P-wave arrivals only is not better; it is actually worse. For a given velocity model and a set of arrival times, RMS is primarily a function of observations: The fewer observations used to locate the earthquake, the lower the RMS is. This resembles the fact that it is easier to fit a small set of observations than a large set of observations. RMS can be used as a measure for location quality but only if the "noise level" of the travel time residuals for a given velocity model

has been estimated. This noise level is a function of the measurement errors and amount of true Earth structure that is not accounted for in the velocity model. One way of assessing the noise level is by computing a so-called minimum 1-D model, which will give a final RMS value of travel time residuals reflecting the noise level contained in the data and in the velocity model (e.g., Kissling 1988, Husen et al. 2003).
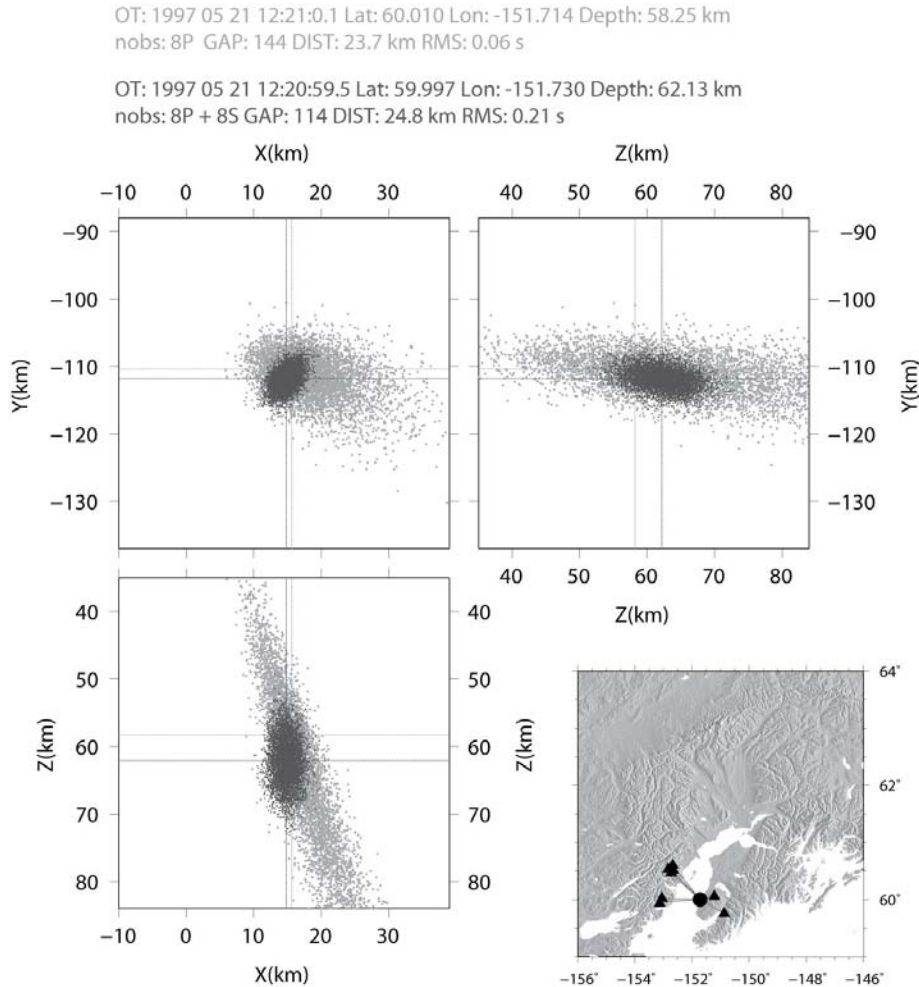
Fig. 4. Earthquake location for an intermediate depth earthquake in the subduction zone in Alaska. Density scatterplots are shown for the location using only P-wave arrivals (grey) and using P- and S-wave arrivals (black). Map in the lower right shows epicenter location (circles) and geometry of stations (black triangles) used to locate the earthquake. The earthquake was located using the NonLinLoc software (*Lomax et al.* 2000) and one dimensional velocity models for P- and S-wave velocities (*van Stiphout et al.* 2009). Note the significant decrease in the formal uncertainties (as represented by the density scatter plots) when S-wave arrivals are used to locate the earthquake. See text for discussion on the effect of S-wave arrivals on earthquake location.

3.2 Accuracy and sources of systematic bias in earthquake locations

The location uncertainties discussed in the previous section are caused by measurements errors and by the unfavorable geometry of stations that recorded the earthquake. The combination of both factors leads to scatter in the earthquake locations that may be quite complicated in shape (e.g., non-ellipsoidal shape). If the measurement errors are known *a priori*, these location uncertainties can be adequately computed using modern location techniques, such as probabilistic direct-search methods. Uncertainties in earthquake locations can also be introduced due to errors in station parameters (location, timing), due to misidentification of seismic phases, and due to errors in the velocity model used to compute the earthquake locations. In general, these errors lead to a systematic bias in earthquake locations and, hence, they affect the accuracy of an earthquake location (e.g., *Jordan and Sverdrup* 1981, *Pavlis* 1986). Moreover, they are difficult to detect and do not follow standard statistical distributions, which makes it difficult to properly account for them in earthquake location. In this section we will discuss two of the most commonly known sources of systematic bias in earthquake location—phase misidentification and velocity model errors—and demonstrate how they can affect earthquake location.

Misidentification of seismic phases

Earthquake location relies heavily on correct phase identification since it tries to minimize residuals between observed and calculated travel times. As such, observed and calculated travel times must correspond to the same phase. Common practice in arrival time data analysis is to assign a certain phase label (*P*, *Pn*, *S*, *Sn*, etc.), which is then used by the location program to compute the corresponding travel time. Assuming a good signal-to-noise ratio, phase identification is generally easy for the first arriving, direct P-wave (often called *Pg*) within the first 60 km of an earthquake location. It becomes complicated, however, at the cross-over distance, where the *Pg* phase and the upper mantle *Pn* phase arrive close in time. Beyond the cross-over distance, the amplitude of the *Pn* phase is small compared to the later arriving *Pg* phase or to the reflection from the Moho (*PmP* phase) and, hence, can be missed in the noise (e.g., *Diehl et al.* 2009b). As a consequence, the secondary *Pg* or *PmP* phase is picked but labeled and used in the location earthquake as a first arriving P-wave. Similarly, the identification of depth phases is difficult for shallow events due to the short time delay relative to the first arriving P-wave (e.g., *Myers et al.* 2009). The correct identification of S-waves is hampered by converted phases which may arrive shortly before the actual S-wave. Therefore, S-wave arrivals should only be picked using all three components, preferably rotated (e.g., *Diehl et al.* 2009a).

Without waveforms, the detection of misidentified phases is difficult. For local and regional distances, arrival times can be plotted in reduced record sections similar to record sections used in refraction seismology. In such plots theoretical arrival times for main crustal phases (*Pg* and *Pn*) can be compared with the observed arrival times and gross inconsistencies can be detected (e.g., *Diehl et al.* 2009b). For example, a secondary arriving *Pg* or *PmP* phase which was picked as a first-arriving *P* phase can be easily be detected beyond the cross-over distance because the phase locates closer to the arrival time branch of the *Pg* or *PmP* phase than to the first arriving *Pn* phase. The usefulness of such an approach for large data sets

is limited since it is laborious to perform this kind of analysis for each earthquake. At the same time, record sections can become quite complicated for regions with significant Moho topography. The differences between theoretical travel times for seismic phases is usually larger than the measurement error of the arrival time picking. Therefore, the arrival time of a phase is an important constraint in phase identification. This can be used to identify phase names by comparing observed arrival times with theoretical arrivals for all phases under consideration. Of course, the success of such an approach depends critically on the quality of the earthquake location and on the quality of the velocity model. One way of accounting for these problems is to invert a high-quality set of arrival times simultaneously for a so-called minimum 1-D model that includes earthquake locations, 1-D seismic velocities and station delays (*Kissling* 1988). Such a model allows us to detect systematic errors in arrival time data by analyzing station delays and travel time residuals (*Maurer et al.* 2010). Another approach used for global data sets is based on travel time probability density functions for a number of phases, including depth phases. *Engdahl et al.* (1998) used these probability density functions to randomly select a phase label according to the probability calculated for each potential phase type. *Myers et al.* (2009) took this approach even further to include phase identification in their Bayesian hierarchical multiple-event seismic location method (*Myers et al.* 2007). This approach mitigates the confounding effects of earthquake location errors and travel time prediction errors in a full probabilistic framework.

On a global scale, the use of probabilistic phase identification yields significantly improved focal depths estimates. This was partly attributed to the use of depth phases (pP, pwP, sP, and PcP) that could be more reliably identified using probabilistic phase identifications (*Engdahl et al.* 1998). On a local and regional scale, the presence of misidentified phases can severely bias earthquake locations. For example, differences in epicenter locations of up to a 30 km were detected in the Alpine region by comparing locations based on routine picks and on revised picks (*Diehl et al.* 2009b). The differences were attributed to the presence of secondary Pg phases that were picked and identified as first-arriving P phases. Similarly, the effect of a single station with wrong coordinates, which in terms of error magnitude can be equivalent to a misidentified phase, can yield location bias of several kilometers (*Maurer et al.* 2010). Whereas the bias in epicenter shows a linear behavior, the bias in focal depth is clearly nonlinear, i.e., no gradual shift is observed in focal depth with increasing distance between true and wrong station coordinates. Fig. 5 shows an example of a Ml=3.4 earthquake recorded at the Swiss Digital Seismic Network that was shifted by 4 km to more shallow depth because of a secondary Pg phases that was picked and identified as first-arriving Pn phase at a single station. The effect is likely so pronounced in the example because phase misidentification occurred at a station that provided an important constraint on focal depth due to the arrival of a Pn phase at this distance. It is also important to note that formal uncertainties as computed by the location pdf do not differ between the two locations. This demonstrates that this kind of error is not reflected in the computation of the formal uncertainties.

The issue of phase identification is less critical for relative location techniques if cross-correlation methods are used to measure delay times. These delay times can

be measured by correlating any phase as long as the same phase is used. For example, a converted phase near the surface can be used equally well as a first arriving S-wave. For cross-correlation measurements it is only important that the same phase is used for all events observed at a common station.
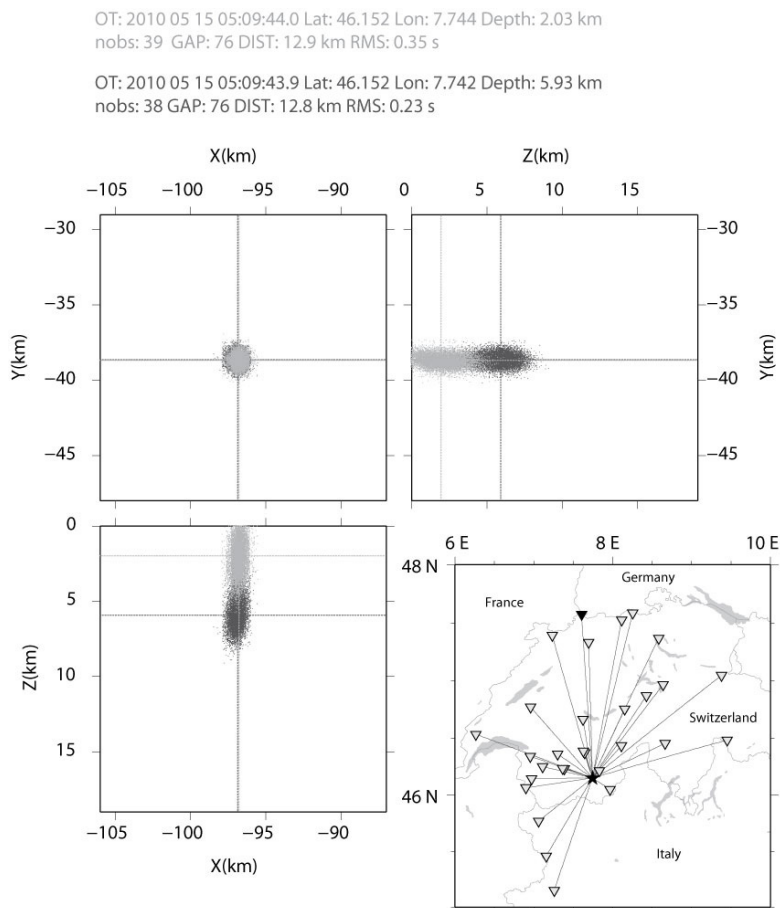
Fig. 5. Density scatterplots of location pdf for an earthquake in Switzerland. The earthquake was located with (grey) and without (dark grey) a misidentified phase. The station with the misidentified phase is shown by a filled black triangle on the map in the lower right. Main location and network parameters for both locations are indicated at the top of the figure. Map in the lower right shows epicenter location (star) and stations (triangles) that were used in the location. The earthquake was located using the NonLinLoc software (*Lomax et al.* 2000) and a 3-D P-wave velocity model (*Husen et al.* 2003). Note the large shift of 4 km to more shallow depth due to a single misidentified phase. Note also that formal uncertainties as given by the density scatter plots do not differ between the locations. See text for more discussion.

Velocity model errors

Pavlis (1986) was one of the first to demonstrate that formal uncertainties as given by traditional error ellipsoids do not reflect uncertainties due to velocity model errors. He concluded that this was due to the fact that velocity model errors do not

follow a Gaussian distribution, which violates the assumptions of the underlying statistics used to compute the formal uncertainties. It is important to note that the distribution of residuals usually follows a Gaussian distribution, which is due to the influence of measurement errors and due to the linearization of the problem (*Pavlis* 1986). This will obscure the true distribution of velocity model errors. Maximal velocity model errors can be estimated as the product of the ray length and the maximum slowness perturbation along the ray path (*Pavlis* 1986). However, this estimate is only valid for small perturbations and it requires an *a priori* knowledge of the maximum slowness perturbations in the real Earth. The approach of *Pavlis* (1986) is still the most complete for appraising velocity model errors, but none of the standard linearized location techniques reflect this. The implementation of *Moser et al.* (1992) to compute the posterior probability density function of the earthquake location (*Tarantola and Valette* 1982) and as implemented in the software package NonLinLoc (*Lomax et al.* 2000) would, theoretically, allow a proper handling of the velocity model errors. However, an *a priori* estimate of the maximum slowness perturbation is still needed.

Knowing that the accuracy of the velocity model is crucial in earthquake location, people have worked on improving seismic velocity models since the beginning of earthquake location. One obvious way of deriving seismic velocity models for earthquake locations is to use a large set of high-quality arrival times from well-constrained earthquake locations. On a global scale this has led to the well-known 1-D velocity models iaspei91 (*Kennett and Engdahl* 1991) and ak135 (*Kennett et al.* 1995). Relocation of well-constrained hypocenter locations indicate that the ak135 model is superior for global earthquake location than the iaspei91 model (*Engdahl et al.* 1998). On a local or regional scale the use of arrival times from well-constrained earthquake locations to derive seismic velocity models for earthquake locations has led to the concept of the minimum 1-D model (*Kissling* 1988). Such a minimum 1-D model is the result of a simultaneous inversion for earthquake locations, seismic velocities, and station delays, thus explicitly solving the coupled hypocenter-velocity problem. To derive a meaningful minimum 1-D model a large range of 1-D velocity models need to be tested (*Kissling et al.* 1994). The resulting minimum 1-D model will represent average seismic velocities for each layer as sampled by the ray distribution; station delays are used to compensate for near-surface velocity heterogeneity underneath the stations and for large-scale systematic variations of seismic velocities such as subducting slabs (e.g., *Husen et al.* 1999). With increasing computational power, people started to compute 3-D velocity models for earthquake locations. These models are usually derived from seismic tomography (for an overview on the method see *Thurber and Ritsema* 2007) and a number of studies have shown the performance of such models compared to 1-D velocity models on different scales (e.g., *Antolik et al.* 2001, *Ritzwoller et al.* 2003, *Husen et al.* 2003). In regions where not enough arrival time data are available to compute 3-D velocity models, other techniques have been applied. A common approach has been to use a 1-D velocity model and apply empirical source-specific station corrections or "correction surfaces" to remove bias due to 3-D Earth structure. This can be done, for example, using high-quality recordings of ground truth events with known locations and a spatial interpolation method such as krigging (e.g., *Myers and Schultz* 2000), or the station terms can be inverted for as part of the earthquake location procedure (e.g. *Richards-Dinger*

and Shearer 2000). Alternatively, velocity models can be compiled from *a priori* information by synthesizing geophysical information that is relevant to the velocity structure, geology, seismicity, and tectonics in the region of interest (e.g., *Flanagan et al.* 2007). No matter which method has been employed to derive a seismic velocity model for earthquake location it is important to note that such a model will be only as good as the quality of the data which were used to compute the model. This means, for example, that the quality of a velocity model can be strongly hampered by the problem of phase misidentification as discussed above. In addition, each model that will be used for earthquake location needs to be validated by relocating sources with known locations, such as explosions, blasts, or so-called ground truth events (e.g., *Husen et al.* 2003, *Yang et al.* 2004).

The effect of velocity model errors on earthquake location accuracy can be large. Using a data set of 156 well-locatable test events from the IASPEI collection of ground truth events *Engdahl* (2006) estimated a location accuracy in epicenter and in focal depth between 9 km and 12 km, and between 9 km and 16 km, respectively. These events were located using a global 1-D velocity model (ak135) and the most accurate results were obtained using the EHB location method that includes the use of later arriving phases and a weighting scheme based on phase variance as a function of distance (*Engdahl et al.* 1998). It can be expected that these estimates will significantly increase for events than are less well-constrained than those used by *Engdahl* (2006). Earthquakes in subduction zones are particularly affected by velocity model errors due to the presence of a dipping high P-wave velocity slab. Earthquake locations shift up to 25 km regionally if they are located using a global 1-D velocity model (iaspei91) that is corrected for 3-D Earth structure compared to locations using the same 1-D velocity model but without corrections; in addition, most epicenters in the circum-Pacific subduction zones are systematically pulled towards the Pacific (*Syracuse and Abers* 2009).

The largest effect of velocity model errors on earthquake location accuracy can be expected for regional and local earthquakes, as arrivals from these earthquakes pass through a highly heterogeneous crust and upper mantle. For example, if a seismic arrival from an earthquake at a distance of about 500 km is misinterpreted with a velocity that is wrong by 5% the distance to the earthquake will be computed incorrectly by about 25 km using that arrival time alone (*Richards et al.* 2006). Fig. 6 shows an example of an explosion in a tunnel in Switzerland that was located 2 km too deep using a regional 3-D P-wave velocity model. The earthquake was mislocated by about 200 m using P-wave velocities derived from the same explosion. These velocities were about 20% slower than those in the regional 3-D model. Moreover, they showed variations in seismic velocities of up to 10% between different stations located between 2 km and 12 km distance from the explosion. This example demonstrates that seismic velocities in the upper crust vary more than we usually think and that a 3-D velocity model does not necessarily yield more accurate earthquake locations.
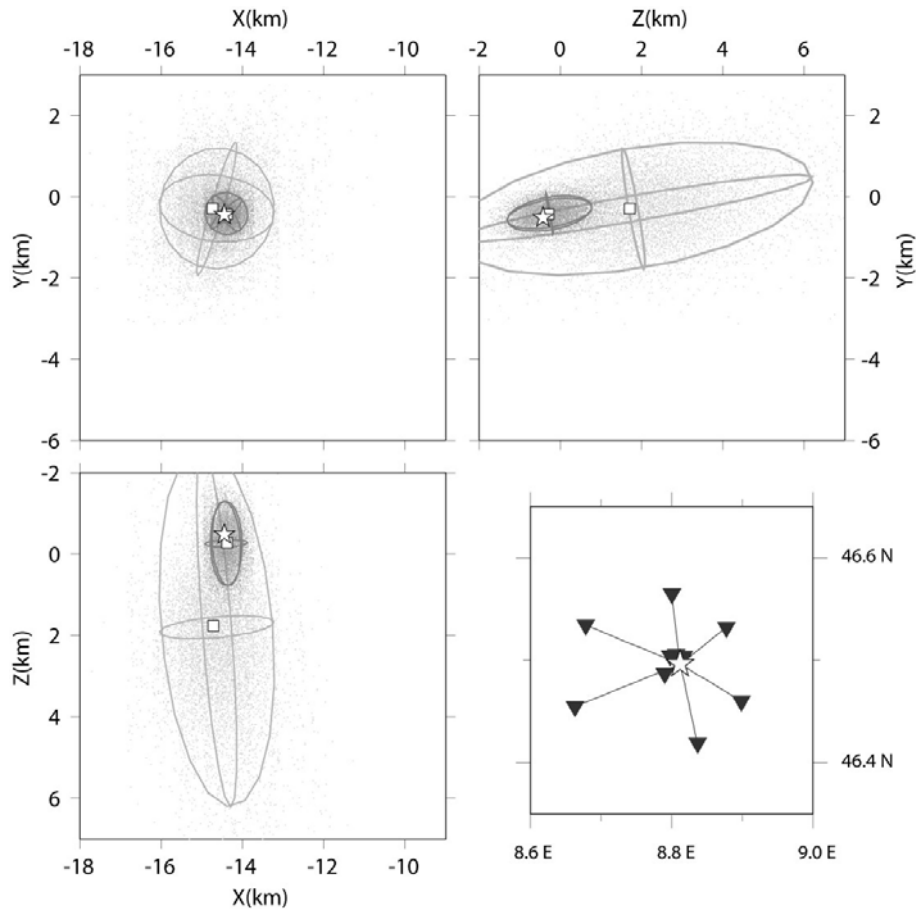
Fig. 6. Density scatterplots of location pdf for an explosion in a tunnel in Switzerland. The explosion was located using a regional 3-D P-wave velocity model (dark grey scatterplots) and using P-wave velocities derived from the explosion. Squares mark maximum likelihood location; true location of the explosion is marked by stars. Error ellipsoids correspond to the 68% confidence ellipsoid as computed from the samples of the location pdf. Map in the lower right shows distribution of stations (triangles) that were used to locate the explosion. Location using the regional 3-D P-wave velocity model is about 2 km too deep but location uncertainties include true location. Using the seismic velocities derived from the explosion the location is only about 200 m too deep. Note that location uncertainties are smaller for this solution since a 2.5 times smaller velocity model error could be used.

4 Choosing a Catalog, and What to Expect

A wide range of earthquake catalogs exist, located with different location techniques, based on different assumptions about the seismic velocity structure, and spanning scales from 10s of km to the entire globe. Each type of catalog has strengths and weaknesses, so there is no one "best" catalog. Choosing the correct catalog for a particular application requires finding the catalog that can best provide the information that will be needed to test the key hypotheses, constrain the important parameters, etc. Once a catalog has been selected, it is important to

keep in mind the potential limitations of the chosen catalog, and explore how these limitations may affect the conclusions of the study.

4.1 Absolute versus Relative Location Accuracy

When choosing between earthquake catalogs based on single-event location methods and catalogs based on relative location techniques, it is important to distinguish between absolute and relative location accuracy and to consider which is the most important for the intended goals of the study. If the primary information required from the catalog is the relative locations of earthquakes, such as the distance between events, a relative location catalog is most likely the best choice. If the study requires a complete catalog, for instance for estimating earthquake rates, a single-event catalog is usually preferable because it will often contain more events than a relative relocation catalog which is limited to clustered events. If the absolute earthquake locations are required, the two types of catalogs can in theory estimate the absolute locations with similar accuracy, although in practice a single-event catalog is often preferable (see also discussion in section 2.3).

Relative location techniques can greatly reduce the formal location error of an earthquake relative to the other earthquakes within the same cluster (*Waldhauser and Schaff* 2008). Applications of relative location techniques exhibit impressive sharpening of clustered seismicity features, compared to single event location catalogs (e.g., *Shearer* 2002, *Richards et al.* 2006). Relative location catalogs are therefore quite useful for studying the geometry of fault systems, and for precise measurement of the distance between successive or neighboring events. Important applications for statistical seismology include studies of the fractal dimension of faulting and characterizing the spatial kernel of earthquake triggering at small scales.

A major drawback for statistical seismology applications is that the relative location catalogs are often not complete down to the same magnitude of completeness as the original network catalogs, and may not be complete at any magnitude. This is because earthquakes that are not strongly linked to other events are usually removed from the inversion because they make the inversion poorly-conditioned. It may be possible to restore these events to the catalog using their single-event locations, but this introduces biases in the relative locations of the restored earthquakes to the linked events, which may defeat the purpose of using a relative location catalog. Single event location catalogs are therefore preferable for applications where a homogeneous complete catalog is needed, such as studies of earthquake rate. An exception is relative location catalogs based on waveform cross-correlation delay times, which may include earthquakes that have an inadequate number of phase picks for single-event location but can be located relative to other events based on the cross-correlation delay times. These catalogs are potentially more complete than single-event location catalogs (e.g., *Waldhauser and Schaff* 2008.)

Single event location catalogs are generally preferable for applications where the absolute earthquake locations are compared to other spatial data, such as mapped faults or geophysical anomalies. *Menke and Schaff* (2004) demonstrated that

relative location techniques can constrain the absolute locations of earthquakes, but no better than single-event locations. Therefore, using a relative location catalog does not add any precision to the comparison with other spatial data, although it sharpens the seismicity features. Single event locations, particularly from nonlinear methods, can provide more informative uncertainty estimates than the linearized relative location methods, for better statistical comparison of locations with other spatial features. Additionally, non-clustered events are often not included in the relative locations catalogs, so these catalogs may provide a biased sample of the earthquake locations.

Relative location catalogs may also be subject to artifacts due to the simplified velocity models that are often used. The publicly available version of the hypoDD double-difference code of *Waldhauser and Ellsworth* (2000), for example, uses a 1-D layered velocity model, and it has been shown that earthquakes can get stuck at the depths of the layer boundaries (*Michilini and Lomax* 2004). In practice, using thinner layers can minimize this type of artifact. The double-difference tomography code tomoDD (*Zhang and Thurber* 2003) can be used for relative relocations in a 3-D velocity model, avoiding location biases that may result from using a 1-D velocity model.

4.2 Spatial Scale

Earthquake location accuracy is often related to the seismic network scale and configuration. Catalogs are typically referred to as local, regional, or global, depending on the scale of the network recording them. Although location techniques in theory are similar irrespective of the scale of the network, in practice different issues arise at different scales. At smaller scales, different phases are not clearly separated in the seismograms, and typically only the first P and possibly S arrivals can be identified and used. At larger scales, arrivals are more clearly separated, and additional reflected and refractive phases and surface waves can be identified and used to constrain the earthquake locations (e.g., *Engdahl et al.* 1998). However, at larger scales, the location uncertainty also increases.

Local earthquake catalogs consist of events recorded at <100 km distance by multiple stations of a local network with station spacing on the order of 10s of km. Usually these catalogs are limited to earthquakes occurring inside the network, that is with an azimuthal gap of <180° given the stations of the network. Locations are based on direct P-wave and S-wave arrival times, usually with many more P-wave times than S-wave times. Formal location uncertainty for earthquakes inside a dense local network (for example, the Southern California Seismic Network) is typically ~1 km horizontally and ~2-3 km in depth. Earthquakes outside the network have considerably higher location uncertainty, and because they are recorded from only one side, there are tradeoffs between the origin times and the location in the direction towards or away from the network (see also discussion in section 3.1). It should also be noted that since larger magnitude earthquakes are recorded out to greater distances, they sample the seismic velocity model deeper than smaller earthquakes. Therefore, if the accuracy of the seismic velocity model varies with depth, larger earthquakes may be artificially offset from smaller events.

Regional catalogs consist of earthquakes recorded at distances on the order of 100s
to 1000s of km. At regional distances, one must be aware of the Pn cross-over
distance, the source-receiver distance at which the Moho refracted wave becomes
the first arrival, rather than the direct P-wave. The cross-over distance is a
function of the Moho depth and the seismic velocity contrast, and varies spatially.
(Typical cross-over distances are around 120 km for 30 km thick crust.) In some
cases, the cross-over distance may also be important in local catalogs, in particular
for deep earthquakes close to the Moho or in regions with strongly varying Moho
depth (e.g., *Diehl et al.* 2009b). At regional distances, phase arrivals are clearly
separated in the seismogram, surface waves are recorded, and the energy is of lower
frequency, all of which allow waveform modeling to be used to constrain the
earthquake location. Waveform modeling is particularly useful in constraining
earthquake depths (e.g. *Zhu and Helmberger* 1996).

Global catalogs consist of earthquakes recorded worldwide. One important class of
phases used in global catalogs is "depth phases", up-going rays that reflect off of the
free surface. A reflected ray then continues to the receiver on a path very similar to
a down-going ray, and the arrival time delay between the down-going and up-going
rays provides a critical constraint on the depth of the earthquake. The formal
location uncertainty of events in a global catalog is typically on the order of 10 km
horizontally and 25 km vertically. The accuracy of the global earthquake locations
can be estimated by relocating earthquakes and explosions for which ground-truth
information is available (e.g., *Bondar et al.* 2004, *Engdahl* 2006). Moreover, the
comparison of earthquake locations for two of the major global catalogs, that of the
International Seismological Centre (ISC) and that of the National Earthquake
Information Center (NEIC), can provide insights into the accuracy of global
earthquake locations. For M≥5 earthquakes, ~95% of ISC and NEIC locations are
within 10 km of each other. Often the depth of a shallow event without depth
phases is poorly constrained, and in these cases the depth is set to a predetermined
depth, which may vary regionally and between catalogs. Typical values are 5 km or
10 km, which often results in horizontal streaks at these depths in vertical cross
sections.

Global centroid catalogs are also sometimes used in statistical studies. The
earthquake centroid, the center of moment, is often offset from the hypocenter by
several 10s of km or more, so the locations from the centroid catalogs are not
directly comparable to hypocenter location catalogs. It is important to choose the
catalog appropriate for the scientific question at hand: if one is interested in where
earthquakes nucleate, a hypocenter catalog is preferable; while if one is interested
in where the most slip occurs, a centroid catalog is more appropriate. The location
uncertainty of centroid catalogs is similar to that of other global location catalogs.

Composite catalogs, made from combining multiple source catalogs, introduce
additional heterogeneity in event locations and accuracy because different agencies
use different techniques and often different velocity models to locate earthquakes.
One approach to limiting heterogeneity, taken by the Advanced National Seismic
System (ANSS) composite catalog, is to consider each contributing catalog as an
authoritative source for a given spatial region. However, this still leaves
considerable heterogeneity, and discontinuities at the boundaries between

authoritative regions. Some regions inside the composite catalog may be outside of each of the contributing networks, and so the earthquakes there may be more poorly located than events in surrounding regions.

4.3 Seismic Velocity Model

Due to the inherent coupling between earthquake locations and seismic velocity, catalogs relocated with different types of seismic velocity models are prone to different location artifacts (see discussion in section 3.2). It is important to remember that the most accurate earthquake locations will be found from the most accurate velocity model. Adding complexity to the model does not necessarily improve its accuracy; a well-constrained 1-D velocity model may produce more accurate earthquake locations than a poorly-constrained 3-D velocity model.

Most earthquake catalogs issued by seismic networks are based on 1-D velocity models. These 1-D models are commonly represented either as a layered model with constant velocity within each specified depth layer, or as a gradient model with linearly increasing velocity with depth within each layer. While the layered models allow quicker ray tracing, sometimes an artifact is created where events get "stuck" at layer boundaries.

The major drawback of 1-D velocity models is that they do not account for lateral variations in the velocity structure. Station corrections can partly account for these lateral velocity variations but in tectonically complex regions with strong Moho topography their application is limited (e.g., *Husen et al.* 2003). One classic example of an artifact from using a 1-D model is the shift in earthquake locations due to an unmodeled lateral velocity contrast across a fault (*Thurber* 1992). For earthquakes that occur along a fault that juxtaposes different lithologies, the travel times to stations on the side of the fault with slower velocity will be relatively longer than the travel times to stations on the faster side. If a 1-D model is used in locating these earthquakes, the earthquakes will appear to be closer to the stations on the fast side of the fault. Such a shift increases with depth, so the earthquakes may appear to define a dipping plane, even if the fault is actually vertical.

There are ways to model lateral velocity variations without constructing a full 3-D velocity model and using 3-D ray tracing. One common approach is to use different 1-D models for stations within different geographical areas (*Oppenheimer et al.* 1993). For example, in the case of the lateral velocity contrast across a fault, a different velocity model could be used for stations on either side of the fault. This approach only works for simple large-scale changes in velocity structure, and becomes impractical if the lateral velocity structure is more complex. Alternatively, if 2D velocity profiles are available from active source seismic experiments, the structure of the profiles can be projected along the direction of local tectonic fabric. However, this approach ignores any out-of-plane velocity variations and ray paths, which may lead to artifacts in both the 2D velocity model and the earthquake locations.

A 3-D velocity model is often derived from the earthquake travel time data in a joint inversion for the velocity model and the earthquake locations (see discussion

in section 3.2). To constrain the velocity model, there must be sufficient ray coverage, and in particular there must be crossing rays, so that the inversion matrix is well-conditioned. Velocity model inversions are usually mixed-determined, with some areas over-determined and some under-determined, and hence require damping and smoothness constraints. Therefore, the (mathematical) resolution of the velocity model is in most places substantially larger than the grid spacing of the velocity model representation. For example, the seismic velocity model of *Hole et al.* (2000) for the San Francisco area is parameterized with a grid spacing of 2 km, but because smoothing was applied on a 12-km length scale, the resolution of this model is not as fine as the parameterization would imply. The models also usually don't have the resolution to image sharp velocity boundaries, and hence ray-tracing in these models may miss important reflections and refractions, which may impact the earthquake locations.

5 Summary, Further Reading, Next Steps

In summary, care should be taken when using earthquake location catalogs in statistical seismology studies, as the catalogs are not exact representations of the true earthquake locations. Instead, earthquake locations are affected by random and systematic errors. Methods to locate earthquake have their strengths and weaknesses, and they rely on certain assumptions. Knowing these will help to choose the correct earthquake catalog.

Acknowledgements

References

Allen, R. (1978), Automatic earthquake recognition and timing from single traces, *Bull. Seismol. Soc. Am.*, 68, 1521-1532.

Antolik, M., G. Ekstrom, and A.M. Dziewonski (2001), Global event location with full and sparse data sets using three-dimensional models of mantle P-wave velocity, *Pure Appl. Geophys.*, 158, 291-317.

Baer, M., and U. Kradolfer (1987), An automatic phase picker for local and teleseismic events, *Bull. Seismol. Soc. Am.*, 77, 1437-1445.

Bakun, W.H., B. Aagaard, B. Dost, W.L. Ellsworth, J.L. Hardebeck, R.A. Harris, C. Ji, M.J.S. Johnston, J. Langbein, J.J. Lienkaemper, A.J. Michael, J.R. Murray, R.M. Nadeau, P.A. Reasenberg, M.S. Reichle, E.A. Roeloffs, A. Shakal, R.W. Simpson and F. Waldhauser (2005), Implications for prediction and hazard assessment from the 2004 Parkfield earthquake, *Nature* 437, 969-974.

Billings, S.D., M.S. Sambridge, and B.L.N. Kennett (1994a), Errors in hypocenter location - picking, model, and magnitude dependence, *Bull. Seism. Soc. Am.*, 84, 1978-1990.

Billings, S.D., B.L.N. Kennet, and M.S. Sambridge (1994b), Hypocenter location - genetic algorithms incorporating problem-specific information, *Geophys. J. Int.*, 118, 693-706.

Bondar, I., S.C. Myers, E.R. Engdahl, and E.A. Bergman (2004), Epicentre accuracy based on seismic network criteria, *Geophys. J. Int.*, 156, **483**-496.

Bormann, P., K. Klinge, and S. Wendt (2002), Data analysis and seismogram interpretation. in *IASPEI New Manual of Seismological Observatory Practice* (*NMSOP*), pp. 100, ed. Bormann, P. GeoForschungsZentrum, Potsdam.

Boyd, T.M., and J.A. Snoke (1984), Error estimates in some commonly used earthquake location programs, *Earthquake Notes*, 55, 3-6.

Buland, R. (1976), The mechanics of locating earthquakes, *Bull. Seismol. Soc. Am.*, 66, 173-187.

Chatelain, J.L., S.W. Roecker, D. Hatzfeld, and P. Molnar (1980), Microearthquake seismicity and fault plane solutions in the Hindu Kush region and their tectonic implications, *J. Geophys. Res.*, 85, 1365-1387.

Deichmann, N., and M. Garcia-Fernandez (1992), Rupture geometry from high-precision relative hypocenter locations of microearthquake clusters, *Geophys. J. Int.*, 110, 501-517.

Deichmann, N., and D. Giardini (2009), Earthquakes induced by the stimulation of an enhanced geothermal system below Basel (Switzerland), *Seismol. Res. Let.*, 80, 784-798.

Di Stefano, R., F. Aldersons, E. Kissling, P. Baccheschi, C. Chiarabba, and D. Giardini (2006), Automatic seismic phase picking and consistent observation error assessment: application to the Italian seismicity *Geophys. J. Int.*, 165, 121.

Diehl, T., N. Deichmann, E. Kissling, and S. Husen (2009a), Automatic S-wave picker for local earthquake tomography, *Bull. Seismol. Soc. Am.*, 99, **1906**-1920.

Diehl, T., E. Kissling, S. Husen, and F Aldersons (2009b), Consistent phase picking for regional tomography models: Application to the greater Alpine region, *Geophys. J. Int.*, 176, 542-554.

Douglas, A. (1967), Joint epicentre determination, *Nature*, 215, 47-48.

Engdahl, E.R. (2006), Application of an improved algorithm to high precision relocation of ISC test events, *Phys. Earth Planet. Int.*, 158, 14-18.

Engdahl, E.R., R. van der Hilst, and R. Buland (1998), Global teleseismic earthquake relocation with improved travel times and procedures for depth determination, *Bull. Seism. Soc. Am.*, 88, 722-743.

Evernden, J.F. (1969), Precision of epicenters obtained by small numbers of world-wide stations, *Bull. Seism. Soc. Am.*, 59, 1365-1398.

Flanagan, M.P., S.C. Myers, and K.D. Koper (2007), Regional travel-time uncertainty and seismic location improvement using a three-dimensional *a priori* velocity model, *Bull. Seism. Soc. Am.*, 97, 804-825.

Flinn, E.A. (1965), Confidence regions and error determinations for seismic event location, *Rev. Geophys.*, 3, 157-185.

Geiger, L. (1912), Probability method for the determination of earthquake epicenters from the arrival time only (translated from German), *Bull. St. Louis Univ.*, 8, 56-71.

Gomberg, J.S., K.M. Shedlock, and S.W. Roecker (1990), The effect of S-Wave arrival times on the accuracy of hypocenter estimation, *Bull. Seism. Soc. Am.*, 80, 1605-1628.

Hole, J. A., T. M. Brocher, S. L. Klemperer, T. E. Parsons, H. M. Benz, and K. P. Furlong (2000), Three-dimensional seismic velocity structure of the San Francisco Bay area, *J. Geophys. Res.* 105, **13,859**–13,874.

Husen, S., and E. Kissling (2001), Local earthquake tomography between rays and waves: fat ray tomography, *Phys. Earth Planet. Int.*, 123, 127-147.

Husen, S., E. Kissling, N. Deichmann, S. Wiemer, D. Giardini, and M. Baer (2003), Probabilistic earthquake location in complex three-dimensional velocity models: Application to Switzerland, *J. Geophys. Res.*, 108, doi: 10.1029/2002JB001778.

Husen, S., E. Kissling, E. Flueh, and G. Asch (1999), Accurate hypocentre determination in the seismogenic zone of the subducting Nazca Plate in northern Chile using a combined on-/offshore network, *Geophys. J. Int.*, 138, 687-701.

Husen, S., and R.B. Smith (2004), Probabilistic earthquake relocation in three-dimensional velocity models for the Yellowstone National Park region, Wyoming, *Bull. Seismol. Soc. Am.*, 94, 880-896.

Jordan, T.H., and K.A. Sverdrup (1981), Teleseismic location techniques and their application to earthquake clusters in the South-Central Pacific, *Bull. Seism. Soc. Am.*, 71, 1105-1130.

Kennett, B.L.N., and E.R. Engdahl (1991), Traveltimes for global earthquake location and phase identification, *Geophys. J. Int.*, 105, 429-465.

Kennett, B.L.N., E.R. Engdahl, and R. Buland (1995), Constraints on seismic velocities in the earth from travel-times, *Geophys. J. Int.*, 122, 108-124.

Kirkpatrick, S., C.D. Gelatt, and M.P. Vechi (1983), Optimization by simulated annealing, *Science*, 220, 671-680.

Kissling, E. (1988), Geotomography with local earthquake data, *Rev. Geophys.*, 26, 659-698.

Kissling, E., W.L. Ellsworth, D. Eberhart-Phillips, and U. Kradolfer (1994), Initial reference models in local earthquake tomography, *J. Geophys. Res*, 99, 19635-19646.

Klein, F.W. (2002). User's Guide to HYPOINVERSE-2000, a Fortran program to solve for earthquake locations and magnitudes, *U.S. Geol. Surv. Open-File Rep.*, 123 pp.

Lahr, J.C. (1989), HYPOELLIPSE: A computer program for determining local earthquake hypocentral parameters, magnitude and first motion pattern (Y2K compliant version), *U.S. Geol. Surv. Open-File Rep.*, 92 pp.

Lay, T., and T. C. Wallace (1995), Modern Global Seismology, Academic Press, International Geophysics Series vol 58.

Lee, W.H.K., and J.C. Lahr (1975), HYPO71 (revised): A computer program for determining hypocenter, magnitude, and first motion pattern of local earthquakes, *U.S. Geol. Surv. Open-File Rep.*, 64 pp. .

Lee, W.H.K., and S.W. Stewart (1981), Principles and applications of microearthquake networks, pp. 293, Academic Press, New York.

Lomax, A. (2005), A reanalysis of the hypocentral location and related observations for the great 1906 California earthquake, *Bull. Seismol. Soc. Am.*, 95, 861-877.

Lomax, A. and A. Curtis (2001), Fast, probabilistic earthquake location in 3-D models using oct-tree importance sampling, *Geophys. Res. Abstracts*, 3:955.

Lomax, A., A. Michelini, and A. Curtis (2008). Earthquake location, direct, global-search methods. in *Encyclopedia of Complexity and System Science*, pp. 2449-2473, ed. Meyers, R. A. Springer, New York.

Lomax, A., J. Virieux, P. Volant, and C. Berge-Thierry (2000), Probabilistic earthquake location in 3-D and layered models, in *Advances in Seismic Event Location*, pp. 101-134, eds. Thurber, C.H. & Rabinowitz, N. Kluwer Academic Publishers, Dordrecht/Boston/London.

Lomax, A., A. Zollo, P. Capuano, and J. Virieux (2001), Precise, absolute earthquake location under Somma-Vesuvius volcano using a new three-dimensional velocity model, *Geophys. J. Int.*, 146, 313-331.

Maurer, H., and U. Kradolfer (1996), Hypocentral parameters and velocity estimation in the western Swiss Alps by simultaneous inversion of P- and S-wave data, *Bull. Seism. Soc. Am.*, 86, 32-42.

Maurer, V., E. Kissling, S. Husen, and R. Quintero (2010), Detection of systematic errors in travel-time data using a minimum 1-D model: Application to Costa Rica seismic tomography, *Bull. Seism. Soc. Am.*, 100, 629-639.

Menke, W. (1989), Geophysical Data Analysis: Discrete Inverse Theory, pp. 289, Academic Press.

Menke, W., and D. Schaff (2004), Absolute earthquake locations with differential data, *Bull. Seism. Soc. Am.*, 94, 2254-2264.

Michelini, A., and A. Lomax (2004). The effect of velocity structure errors on double-difference earthquake location, *Geophys. Res. Lett.*, 31, L09602. doi:10.1029/2004GL019682.

Milne, J. (1886). Earthquakes and Other Earth Movements, Appelton, New York.

Moser, T.J., T. van Eck, and G. Nolet (1992), Hypocenter determination in strongly heterogeneous earth models using the shortest path method, *J. Geophys. Res*, 97, 6563-6572.

Myers, S.C., G. Johannesson, and W. Hanley (2007), A Bayesian hierarchical method for multiple-event seismic location, *Geophys. J. Int.*, 171, 1049-1063.

Myers, S.C., G. Johannesson, and W. Hanley (2009), Incorporation of probabilistic seismic phase labels into a Bayesian multiple-event seismic locator, *Geophys. J. Int.*, 177, 193-204.

Myers, S.C., and C.A. Schultz (2000), Improving sparse network seismic location with Bayesian kriging and teleseismically constrained calibration events, *Bull. Seism. Soc. Am.*, 90, 199-211.

Nelson, G.D., and J.E. Vidale (1990), Earthquake locations by 3-D finite-difference travel times, *Bull. Seism. Soc. Am.*, 80, 395-410.

Oppenheimer, D., F. Klein, J. Eaton, and F. Lester (1993), The Northern California Seismic Network Bulletin January - December 1992, USGS Open-File Report 93-578.

Pavlis, G.L. (1986), Appraising earthquake hypocenter location errors - a complete, practical approach for single-event locations, *Bull. Seism. Soc. Am.*, 76, 1699-1717.

Pujol, J. (1992), Joint hypocentral location in media with lateral velocity variations and interpretation of the station corrections, *Phys. Earth Planet. Int.*, 75, 7-24.

Pujol, J. (2000), Joint event location - The JHD technique and applications to data from local seismic networks. in *Advances in Seismic Event Location*, eds. Thurber, C. H. & Rabinowitz, N. Kluwer Academic Publishers, Dordrecht/Boston/London.

Reid, H.F. (1910), The Mechanics of the Earthquake, Vol. II of The California Earthquake of April 18, 1906. in *Report of the State Earthquake Investigation Commisision*, ed Lawson, A. C. Carnegie Institution of Washington.

Richards, P.G., F. Waldhauser, D. Schaff, and W.Y. Kim (2006), The applicability of modern methods of earthquake location, *Pure Appl. Geophys.*, 163, 351-372.

Richards-Dinger, K.B. and P.M. Shearer (2000), Earthquake locations in southern California obtained using source specific station terms, *J. Geophys. Res.*, 105, 10,939-10,960.

Ritzwoller, M.H., N.M. Shapiro, A.L. Levshin, E.A. Bergman, and E.R. Engdahl (2003), Ability of a global three-dimensional model to locate regional events, *J. Geophys. Res.*, 108. doi:10.1029/2002jb002167.

Rowe, C.A., R.C. Aster, B. Borchers, and C.J. Young (2002), An automatic, adaptive algorithm for refining phase picks in large seismic data sets, *Bull. Seism. Soc. Am.*, 92, 1660-1674.

Rubin, A.M., and D. Gillard (2000), Aftershock asymmetry/rupture directivity among central San Andreas fault microearthquakes, *J. Geophys. Res.*, 105, 19,095-19,109

Sambridge, M., and G. Drijkoningen (1992), Genetic algorithms in seismic waveform inversion, *Geophys. J. Int.*, 109, 323-342.

Sambridge, M., and K. Gallagher (1993), Earthquake hypocenter location using genetic algorithms, *Bull. Seism. Soc. Am.*, 83, 1467-1491.

Sambridge, M., and B.L.N. Kennett (1986), A novel method for hypocentre location, *Geophys. J. R. Astron. Soc.*, 87, 679-697.

Sambridge, M., and K. Mosegaard (2002). Monte Carlo methods in geophysical inverse problems, *Rev. Geophys.*, 40, 3.1-3.29. doi: 10.10129/2000RG000089.

Schaff, D.P., G.H.R. Bokelmann, W.L. Ellsworth, E. Zanzerkia, F. Waldhauser, and G.C. Beroza (2004), Optimizing correlation techniques for improved earthquake location, *Bull. Seism. Soc. Am.*, 94, 705-721.

Shearer, P.M. (1999), Introduction to Seismology, Cambridge University Press.

Shearer, P.M. (2002), Parallel fault strands at 9-km depth resolved on the Imperial Fault, Southern California, *Geophys. Res. Lett.*, 29(14). doi:10.1029/2002GL015302.

Syracuse, E.M., and G.A. Abers (2009), Systematic biases in subduction zone hypocenters, *Geophys. Res. Lett.*, 36. doi:10.1029/2009gl037487.

Tarantola, A. (2005), Inverse problem theory and methods for model parameter estimation, *SIAM*.

Tarantola, A., and B. Valette (1982), Inverse problems = quest for information, *J. Geophys.*, 50, 159-170.

Thurber, C.H., and J. Ritsema (2007), Theory and observations - seismic tomography and inverse methods. in *Treatise on Geophysics*, pp. 323-375, ed. Schubert, G. Elsevier.

Thurber, C.H. (1992), Hypocenter velocity structure coupling in local earthquake tomography, *Phys. Earth Planet. Int.*, 75, 55-62.

Thurber, C.H. (1993), Local earthquake tomography: Velocities and Vp/Vs theory. in *Seismic Tomography. Theory and Practive*, pp. 563-583, eds. Iyer, H. M. & Hirahara, K. Chapman and Hall, New York.

van Stiphout, T., E. Kissling, S. Wiemer, and N. Ruppert (2009), Magmatic processes in the Alaska subduction zone by combined 3-D b-value imaging and targeted seismic tomography, *J. Geophys. Res.*, 114. doi:10.1029/2008jb005958.

Waldhauser, F., and W.L. Ellsworth (2000), A double-difference earthquake location algorithm: Method and application to the northern Hayward fault, California, *Bull. Seismol. Soc. Am.*, 90, 1353-1368.

Waldhauser, F., and D.P. Schaff (2008), Large-scale relocation of two decades of Northern California seismicity using cross-correlation and double-difference methods, *J. Geophys. Res.*, 113, B08311, doi:10.1029/2007JB005479.

Wilcock, W.S.D., and D.R. Toomey (1991), Estimating hypocentral uncertainties for marine microearthquake surveys: A comparison of the generalized inverse and grid search methods, *Marine Geophys. Res.*, 13, 161-171.

Wittlinger, G., G. Herquel, and T. Nakache (1993), Earthquake location in strongly heterogeneous media, *Geophys. J. Int.*, 115, 759-777.

Wolfe, C.J. (2002), On the mathematics of using difference operators to relocate earthquakes, *Bull. Seism. Soc. Am.*, 92, 2879-2892.

Yang, X.P., I. Bondar, J. Bhattacharyya, M. Ritzwoller, N. Shapiro, M. Antolik, G. Ekstrom, H. Israelsson, and K. McLaughlin (2004), Validation of regional and teleseismic travel-time models by relocating ground-truth events, *Bull. Seism. Soc. Am.*, 94**,** 897-919.

Zeiler, C. and A.A. Velasco (2009), Seismogram picking error from analyst review (SPEAR): single-analyst and institution analysis, *Bull. Seism. Soc. Am.*, 99**,** 2759-2770.

Zhang, H., and C.H. Thurber (2003), Double-difference tomography: the method and its application to the Hayward fault, California, *Bull. Seismol. Soc. Am.*, 93, 1875-1889.

Zhang, H., C.H. Thurber, and P. Bedrosian (2009), Joint inversion for Vp, Vs, and Vp/Vs at SAFOD, Parkfield, California, *Geochem. Geophys. Geosyst.*, 10, Q11002, doi:10.1029/2009GC002709.

Zhu, L., and D.V. Helmberger (1996), Advancements in source estimation techniques using broadband regional seismograms, *Bull. Seismol. Soc. Am.*, 86, 1634-1641.